



Analysis of global methane changes after the 1991 Pinatubo volcanic eruption

N. Bândă^{1,2}, M. Krol^{3,4,1}, M. van Weele², T. van Noije², and T. Röckmann¹

¹Institute for Marine and Atmospheric Research Utrecht, Utrecht University, Utrecht, The Netherlands

²Royal Netherlands Meteorological Institute (KNMI), De Bilt, The Netherlands

³Dept. of Meteorology and Air Quality, Wageningen University and Research Center, Wageningen, The Netherlands

⁴Netherlands Institute for Space Research (SRON), Utrecht, The Netherlands

Correspondence to: N. Bândă (n.l.banda@uu.nl)

Received: 21 June 2012 – Published in Atmos. Chem. Phys. Discuss.: 19 July 2012

Revised: 17 December 2012 – Accepted: 8 February 2013 – Published: 27 February 2013

Abstract. The global methane (CH₄) growth rate showed large variations after the eruption of Mount Pinatubo in June 1991. Both sources and sinks of tropospheric CH₄ were altered following the eruption, by feedback processes between climate and tropospheric photochemistry. Such processes include Ultra Violet (UV) radiative changes due to the presence of volcanic sulfur dioxide (SO₂) and sulphate aerosols in the stratosphere, and due to stratospheric ozone depletion. Changes in temperature and water vapour in the following years caused changes in tropospheric chemistry, as well as in natural emissions. We present a sensitivity study that investigates the relative effects that these processes had on tropospheric CH₄ concentrations, using a simple one-dimensional chemistry model representative for the global tropospheric column. To infer the changes in UV radiative fluxes, the chemistry model is coupled to a radiative transfer model. We find that the overall effect of natural processes after the eruption on the CH₄ growth rate is dominated by the reduction in CH₄ lifetime due to stratospheric ozone depletion. However, all the other processes are found to have non-negligible effects, and should therefore be taken into account in order to obtain a good estimate of CH₄ concentrations after Pinatubo. We find that the overall effect was a small initial increase in the CH₄ growth rate after the eruption, followed by a decrease of about 7 ppb yr⁻¹ by mid-1993. When changes in anthropogenic emissions are employed according to emission inventories, an additional decrease of about 5 ppb yr⁻¹ in the CH₄ growth rate is obtained between the years 1991 and 1993. The results using the simplified single column model are in good qualitative agree-

ment with observed changes in the CH₄ growth rate. Further analysis, taking into account changes in the dynamics of the atmosphere, variations in emissions from biomass burning, and in biogenic emissions of non-methane volatile organic compounds (NMVOC), requires the use of a full three-dimensional model.

1 Introduction

CH₄ is the second most abundant anthropogenic greenhouse gas in the atmosphere after CO₂. Its concentration in the atmosphere has increased since preindustrial times by a factor of 2.5 (Dlugokencky et al., 2011). A good understanding of the processes responsible for variations in the CH₄ concentration is needed for making future predictions and developing mitigation strategies. However, the evolution of the CH₄ concentrations observed in the background atmosphere in the past three decades is not fully understood (Montzka et al., 2011a). The growth rate of CH₄ was generally positive and showed a decreasing trend during the 80s and 90s, with year to year fluctuations (Dlugokencky et al., 2003). As shown in Fig. 7, particularly large fluctuations were observed in the years following the eruption of Mount Pinatubo in 1991 (Dlugokencky et al., 1994, 1996; Bekki and Law, 1997; Butler et al., 2004; Bousquet et al., 2006). After a peak of about 16 ppb yr⁻¹ near the time of the eruption, the globally averaged CH₄ growth rate dropped to -2 ppb yr⁻¹ in late 1992, remaining negative for the second half of the year 1992 (Dlugokencky et al., 2003). A subsequent recovery of

the growth rate to 7 ppb yr^{-1} was observed by the end of 1993.

Changes in the global CH_4 concentration are determined by either changes in CH_4 emissions or by changes in the CH_4 lifetime. CH_4 is emitted from both natural sources (e.g. wetlands, oceans and geological seeps) and anthropogenic sources (e.g. agriculture, fossil fuel exploitation, waste treatment and biomass burning). The lifetime of CH_4 in the atmosphere is determined by the reaction of CH_4 with the hydroxyl radical (OH) in the troposphere, by the uptake of CH_4 by soils and by the destruction of CH_4 in the stratosphere. The main sink is, however, the reaction with OH, the other processes contributing by only 10–15 % to the CH_4 loss (Prather et al., 2001; Spahni et al., 2011). Atmospheric levels of OH are determined by tropospheric photolysis reactions driven by the incident solar UV radiation, by water vapour levels, and by non-linear tropospheric chemistry. Because OH reacts with these species, its abundance is sensitive to atmospheric concentrations of CH_4 , nitrogen oxides (NO_x), carbon monoxide (CO) and NMVOC. Montzka et al. (2011b) showed by inversions of methyl chloroform that global tropospheric OH is relatively stable to perturbations, having an interannual variability of $2.3 \pm 1.5 \%$ for the period 1998 to 2007. Such a small variability was shown to be consistent with the small interannual variability in CH_4 concentrations. In a previous study, Prinn et al. (2005) found an interannual variability in tropospheric OH of 7 to 9 % for the period 1978 to 2004. On a decadal timescale, a possible small positive trend in OH of the order of 0.2 \% yr^{-1} for the period 1985 to 2000, and higher after the year 2000, has been suggested by inversions of CH_4 and $\delta^{13}\text{C-CH}_4$ (Monteil et al., 2011, scenario P2).

The eruption of Mount Pinatubo triggered a multitude of photochemical effects (McCormick et al., 1995), including feedbacks between climate and atmospheric photochemistry, which contributed to the observed evolution of the CH_4 concentrations. The different processes had both positive and negative impacts on the CH_4 growth rate, affecting CH_4 emissions and the CH_4 lifetime. From satellite observations it is estimated that the eruption emitted about $18 \pm 4 \text{ Tg SO}_2$ (Guo et al., 2004a). Volcanic SO_2 absorbs UV radiation between 290 nm and 330 nm, thus its presence in the stratosphere would lead to a decrease in ozone photolysis in the troposphere (Dlugokencky et al., 1996). Since OH formation in the troposphere depends on the photolysis of ozone to $\text{O}(^1\text{D})$, the UV absorption by SO_2 would lead to a longer CH_4 lifetime. SO_2 stayed in the stratosphere for a few months, forming sulphate aerosols with an e-folding time of 23–25 days (Guo et al., 2004a). Enhanced sulphate aerosols were observed by the SAGE II satellite instrument for up to 4 yr after the eruption at heights between 15 and 30 km with a maximum globally averaged aerosol optical depth (AOD) at 550 nm of approximately $\tau = 0.15$ about 7 months after the eruption (Russell et al., 1996; Thomason et al., 1997). Scattering of solar radiation by sulphate aerosols would lead

to a further reduction of photolysis frequencies in the troposphere, thus to a longer CH_4 lifetime. Particles of ash emitted directly by the eruption would also absorb and scatter solar radiation, determining a similar effect on CH_4 lifetime. However, because of their lifetime of only a few days, they are considered to have a negligible global impact (Guo et al., 2004b; Niemeier et al., 2009) and are not included in our study.

Another secondary effect on the CH_4 lifetime is triggered by the destruction of stratospheric ozone on sulphate aerosols. A maximum global ozone depletion of 5 % was observed by TOMS about two years after the eruption (Chipperfield et al., 2003). Changes of similar magnitude have been obtained in modelling studies (Kinnison et al., 1994; Bekki and Pyle, 1994), and were attributed to enhanced heterogeneous ozone-depleting reactions on sulphate aerosols and changes in circulation due to stratospheric aerosol heating. Stratospheric ozone loss would lead to an increase of UV radiation in the troposphere, and thus to a higher OH abundance and a shorter CH_4 lifetime.

The eventual fate of the volcanic sulfur is deposition to the surface. The modelling results of Gauci et al. (2008) indicate that deposition of 122 Tg SO_2 emitted by the Laki eruption led to a decrease of 8.8 Tg yr^{-1} in CH_4 emissions from wetlands in the two years following the eruption. As a rough estimate assuming linearity, the Pinatubo eruption would lead to 1.3 Tg decrease in the emissions. We consider this effect to be small and do not investigate it further here.

Other effects of the eruption on CH_4 concentrations have occurred because of temperature changes after the eruption (Bekki and Law, 1997). The scattering of shortwave radiation by aerosols led to an increase in the reflected solar radiation of up to 10 W m^{-2} at the top of the atmosphere (Bender et al., 2010). This affected tropospheric temperatures, leading to an observed global cooling of up to 0.45 K in the two years following the eruption (Free and Angell, 2002). Bender et al. (2010) show that ten general circulation models give a maximum decrease of 0.5 K in response to the observed changes in the shortwave radiative flux after the eruption. They attribute the 0.05 K difference between models and observations to the coinciding El Niño event.

Temperature perturbations trigger changes in the chemical composition of the atmosphere, as well as in natural sources related to biogenic activity. A decrease in temperature would generally slow down photochemical transformations. In particular, the slowdown of the reaction between CH_4 and OH would lead to higher tropospheric CH_4 concentrations (Bekki and Law, 1997). Soden et al. (2002) found that the cooling after the eruption is associated to a maximum global decrease of 3 % in the water vapour column in both observations and model simulations. Less water vapour in the troposphere would imply less OH formation by photolysis of ozone, because the reaction between $\text{O}(^1\text{D})$ and water becomes less likely. This would increase the CH_4 lifetime, leading to CH_4 build-up in the atmosphere.

Natural emissions from wetlands, accounting for about 30% of the total emissions in the year 2004 (Spahni et al., 2011), are sensitive to temperature and soil moisture changes. Furthermore, natural emissions of NMVOC are known to be temperature dependent (Guenther et al., 1993). A decrease in the surface temperature would result in reductions in both CH₄ emissions from wetlands and biogenic NMVOC emissions. Biogenic emissions of NMVOC are also dependent on the amount of photosynthetically active radiation (PAR) reaching the surface (Guenther et al., 1993). Decrease in PAR fluxes because of enhanced aerosol scattering would further decrease these emissions. While a reduction in CH₄ emissions directly impacts CH₄ concentrations, a decrease in NMVOC emissions may affect OH, and thus impose an indirect impact on the CH₄ lifetime.

The eruption of Pinatubo also changed the dynamics of the atmosphere, which might have influenced OH and CH₄ concentrations. It was inferred in the 4-box modelling study of Schauffler and Daniel (1994) that heating of the stratosphere may increase the exchange between the stratosphere and the troposphere, leading to a decrease in tropospheric CH₄ concentrations. Lowe et al. (1997) suggest that a large effect of enhanced stratosphere-troposphere exchange would be inconsistent with the decrease in observed $\delta^{13}\text{C}$ in this period. However, other isotope data from this period do not support a strong decrease in $\delta^{13}\text{C}$ between 1991 and 1992 (Quay et al., 1999).

Although the processes presented above are known to have contributed to the evolution of the CH₄ growth rate after the Pinatubo eruption, their relative magnitudes are not yet totally resolved. CH₄ observations show the net outcome of these processes and other processes not related to the eruption, such as changes in anthropogenic emissions. The growth rate changes after the eruption have been attributed in other studies to changes in either sources or sinks. Dlugokencky et al. (1996) show that the evolution of CH₄ and CO in 1991 and early 1992 is consistent with a decrease in OH for up to one year after the eruption. They relate this decrease in OH to an attenuation of the UV flux due to the presence of SO₂ and sulphate in the stratosphere. Additionally, Dlugokencky et al. (1994) relate the decrease in CH₄ growth rate in 1992 to a decrease in anthropogenic emissions due to the collapse of the Soviet Union. The modelling study of Bekki and Law (1997) shows that temperature-related effects had a significant impact on the growth rate of CH₄ in 1991–1992. They find that reduced emissions from wetlands may partly or fully explain the reduced growth rate in 1992. The inverse modelling study of Butler et al. (2004) reveals a global source-sink imbalance of +27 Tg CH₄ for the year 1991 and –19 Tg for the year 1992. In their inverse modelling studies, Bousquet et al. (2006) and Wang et al. (2004) both find a decrease in wetland emissions of 20–25 Tg between 1991 and 1993. Bousquet et al. (2006) also find reductions in the biomass burning and anthropogenic emissions, as well as in the OH sink for this period. In contrast, Wang et al.

(2004) postulate an increase in OH due to reduced stratospheric ozone. Using a two-dimensional model, Bekki et al. (1994) also conclude that half of the CH₄ growth rate reduction in 1992 can be attributed to the effect of decreased stratospheric ozone. In the modelling study of Telford et al. (2010) it is found that natural isoprene emissions have a minimum in early 1993, yielding an increase in the CH₄ sink of 5 Tg yr⁻¹. Telford et al. (2010) also show that variations in meteorology lead to a decrease in the CH₄ sink of up to 14 Tg yr⁻¹, mainly due to changes in temperature and water vapour following the eruption. To our knowledge, no complete study has been made to include all competing effects of the Pinatubo eruption and to analyse the processes responsible for OH and CH₄ growth rate variations. Quantifying these processes may help us gain a better understanding of the CH₄ budget and, consequently, to make better predictions of the future atmospheric burdens.

In this sensitivity study we will use a simplified tropospheric column chemistry model as a first step to assess the changes in the CH₄ growth rate after the Pinatubo eruption and the relative contributions of the various processes. First, we will analyse how the equilibrium state of the chemical system changes when varying individual conditions (emissions, photolysis frequencies, water vapor). The impact on the tropospheric steady state gives us an idea about the drivers of CH₄ and OH concentrations, and about the relative magnitude of different processes. Next, we allow the system to respond to transient perturbations. The response of CH₄ concentrations to natural changes after the eruption will be contrasted to their response to changes in anthropogenic emissions. Due to obvious limitations of a single column model, the effect of changes in the dynamics of the atmosphere cannot be studied here. Additionally, because of the high sensitivity of OH to isoprene emissions in our model (see Sect. 3.1.1), we do not include the effect of changes in NMVOC emissions.

A detailed description of the column chemistry model is presented in Sect. 2. In Sect. 3.1 we show sensitivities of the model, and evaluate its performance in representing the global atmosphere in the period 1890–2005. We show our results on steady-state and transient CH₄ changes after Pinatubo in Sect. 3.2, and conclusions are drawn in Sect. 4.

2 Model setup

The model used in this study is a one-dimensional column chemistry model, coupled to the radiation model TUV (Madronich (1993), <http://cprm.acd.ucar.edu/Models/TUV/>). The chemistry model can be used both in steady-state and transient versions. The effects of atmospheric perturbations on photolysis frequencies are calculated with the radiative transfer model TUV, and then employed in the chemistry model.

Table 1. Reactions included in the model. Reaction rate coefficients are the ones described in Huijnen et al. (2010), except for photolysis rates, which are computed using TUV.

Reactants	Products
$O_3 + h\nu$	$2 \times OH$
$NO_2 + h\nu$	$O_3 + NO$
$O_3 + NO$	NO_2
$O_3 + OH$	HO_2
$O_3 + HO_2$	OH
$HO_2 + HO_2$	
$HO_2 + OH$	
$HO_2 + NO$	$OH + NO_2$
$NO_2 + OH$	
$CO + OH$	HO_2
$CH_4 + OH$	$0.9 \times CO + RO_2$
$RH + OH$	$0.35 \times CO + RO_2$
$RO_2 + NO$	$NO_2 + y \times HO_2$
$RO_2 + HO_2$	
$RO_2 + RO_2$	

2.1 The column chemistry model

In this exploratory study we use a strongly simplified model that represents the troposphere in 10 vertical layers of 1.5 km thickness each. The chemical scheme employs 8 chemical species, of which 5 are transported between adjacent layers (O_3 , NO_x , CH_4 , CO , RH). OH , HO_2 and RO_2 are not transported, but calculated in steady state with the longer-lived transported species. Here RH stands for NMVOC, and RO_2 for peroxy-radicals formed from NMVOC and CH_4 oxidation.

Vertical transport is defined by vertical diffusion coefficients of $10 \text{ m}^2 \text{ s}^{-1}$ between the first two layers (at 1.5 km), $5 \text{ m}^2 \text{ s}^{-1}$ between the second and 3rd layers (at 3 km) and $2 \text{ m}^2 \text{ s}^{-1}$ higher up. No flux to the stratosphere is considered except for ozone and CH_4 . For ozone, we fix the concentration in the upper layer (at 13.5 km) at 148 ppb. A flux of 40 Tg yr^{-1} to the stratosphere is considered for CH_4 , following Prather et al. (2001).

The chemical reactions included are presented in Table 1. We run the model with all-day all-year averaged reaction rate coefficients and photolysis frequencies. The 0.9 CO yield from CH_4 oxidation is comparable to that found by complex 3-D global chemistry models (Shindell et al., 2006). The yield of CO from the oxidation of NMVOC varies strongly between species (Grant et al., 2010). We use here a global CO yield from NMVOC of 0.35. CH_4 oxidation produces CH_3O_2 , which may react with NO , yielding at least one molecule of HO_2 through all the reaction pathways. CH_3O_2 is included in the model as RO_2 , together with other compounds produced from NMVOC oxidation. Thus we consider an HO_2 yield y from the reaction of RO_2 and NO , equal to the ratio between the CH_3O_2 production from CH_4 and the total

RO_2 production. For computational reasons, we use a global yield determined from a steady-state assumption. The rate of production of CH_3O_2 from CH_4 oxidation is equal to the rate of loss of CH_4 in this reaction. Assuming steady state, this is equal to the emission rate of CH_4 (E_{CH_4}). Similarly, the rate of RO_2 production from NMVOC is equal to the emission rate of NMVOC (E_{RH}). Therefore the HO_2 yield y from the reaction of RO_2 and NO is taken as $\frac{E_{CH_4}}{E_{CH_4} + E_{RH}}$.

Dry deposition of ozone and NO_2 are included with a deposition velocity of $1.0 \times 10^{-3} \text{ m s}^{-1}$. An additional loss of NO_2 through heterogeneous reactions is considered, with a deposition velocity of $1.5 \times 10^{-4} \text{ m s}^{-1}$ throughout the column.

A time-dependent version of the chemistry model performs transient simulations using the Euler Backward Iterative scheme with a time step of one hour.

2.2 Photolysis frequencies

The TUV model version 4.1 is used to calculate the effects of SO_2 , aerosols and ozone column on tropospheric photolysis frequencies. Yearly averaged photolysis frequencies are calculated by averaging daily mean photolysis frequencies at 30°N for the 15th of the months of March, June, September and December. This latitude band is used because photochemistry is most active in the tropics, and is chosen such that CH_4 concentrations and lifetime are realistically reproduced.

For the base scenario, the climatological aerosol profile of Elterman (1968) is used, with an aerosol single scattering albedo of 0.99.

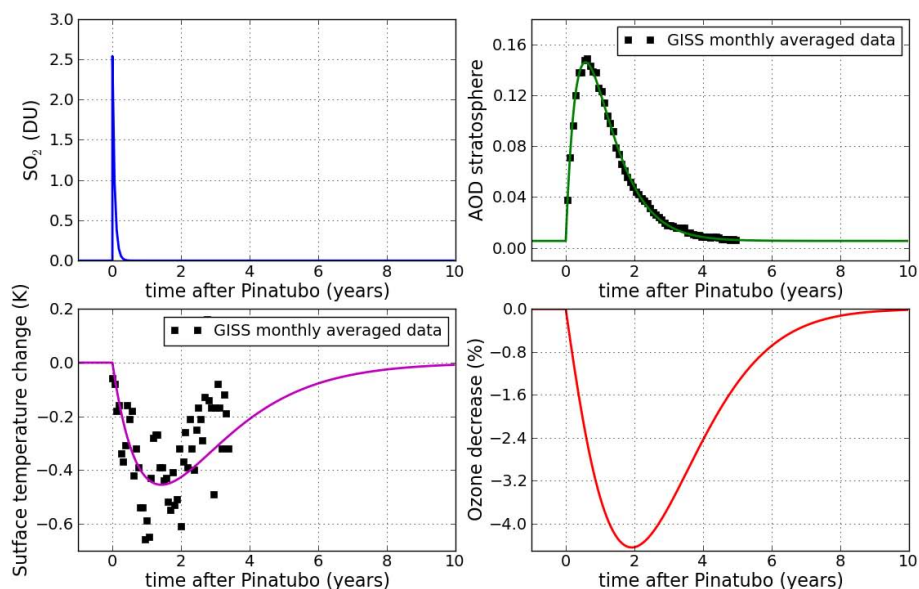
2.3 Emissions and atmospheric parameters

Global anthropogenic emissions for NO_x , CO , CH_4 and NMVOCs are taken from EDGAR 4.1 yearly values for the years 1970–2005 (European Commission and Joint Research Centre (JRC)/Netherlands Environmental Assessment Agency (PBL), 2010), and EDGAR-HYDE decadal emissions for the years 1890–1970 (Van Aardenne et al., 2001). Natural emissions used are described in Huijnen et al. (2010), except for CH_4 emissions, which are taken from Spahni et al. (2011) posterior values for the year 2004. The evolution of CH_4 emissions implemented in the model is shown in Fig. 4. In addition to surface NO_x emissions, we add yearly 6.3 Tg N of NO_x from lightning (Huijnen et al., 2010), evenly distributed throughout the column in terms of mixing ratios.

Profiles of temperature, water vapour, ozone, and air density for 30°N were derived from the global 3-D chemistry transport model TM5 (Huijnen et al., 2010) driven by ERA-Interim meteorological fields (Dee et al., 2011) for the year 2005. These are applied both in TUV and in the column chemistry model. The ozone columns for the four months used here are respectively 302, 294, 283 and 270 Dobson Units (DU).

Table 2. Setup of the Pinatubo simulations. AOD = aerosol optical depth; DU = Dobson Unit.

Simulation name	Changes implemented in TUV	Changes implemented in the column chemistry model
SO ₂	2.54 DU of SO ₂ between 15 and 30 km altitude	Changes in photolysis frequencies from TUV
Aerosol	0.15 AOD due to Pinatubo between 15 and 30 km altitude	Changes in photolysis frequencies from TUV
Ozone	5 % ozone column decrease	Changes in photolysis frequencies from TUV
Temp Rates		Changed reaction rate coefficients due to temperature
H ₂ O		Changes in water vapour profile due to changed temperature profile
CH ₄ Emis		Changes in CH ₄ emissions from wetlands due to temperature
Temp All		Changes in reaction rate coefficients, water vapour and CH ₄ emissions due to temperature

**Fig. 1.** Time evolution of the forcings, as implemented in the model. Squares represent monthly averaged GISS data (Hansen et al., 2005, 2010).

2.4 Implementation of Pinatubo perturbations

We define two sets of simulations. First, we evaluate the change in the model state due to individual natural perturbations after the eruption, in order to distinguish the most important drivers of CH₄ concentrations. In the second set of simulations we also include variations in anthropogenic CH₄ sources, with the aim to reproduce the evolution of the global CH₄ concentration in the early 1990s.

In the first set of simulations, we define the base simulation as the 1990 equilibrium situation. Next, the change in the model state due to the natural perturbations after Pinatubo is evaluated as a steady-state and as a transient response. The perturbations implemented in TUV and the column chemistry model are summarised in Table 2. In these sensitivity experiments, we assume constant anthropogenic and biomass burning emissions.

To compute the perturbations in photolysis frequencies after Pinatubo in TUV, we implement single forcings of 5 % decrease in ozone column, 2.54 DU increase in SO₂, equivalent to 18.5 Tg SO₂, and 0.15 increase in AOD. SO₂ and aerosols are considered to be evenly distributed in our atmospheric column between 15 and 30 km altitude. In the column chemistry model, the perturbations in photolysis frequencies are then scaled with the magnitudes of the forcings, thus assuming that the effects of these processes are linear. In addition, we assume additivity between the different processes by adding the perturbations in photolysis frequencies when more than one process is considered. We tested the effect of this assumption on our results by performing two simulations: one in which we used photolysis rates calculated with TUV by implementing all the forcings at the same time, and one in which we implemented each forcing separately and assumed additivity. The difference in the CH₄ steady-state concentration between the two simulations is 0.5 ppb, which is small compared to the magnitude of the perturbations related to the eruption.

The time evolution of the forcings assumed in the column chemistry model is based on observed values, and is shown in Fig. 1. For SO_2 , an exponential decay with an e-folding time of 24 days is considered, as found by Guo et al. (2004a), and a starting global mean concentration of 2.54 DU directly after the eruption. For the aerosol optical thickness, we use the Goddard Institute for Space Studies (GISS) monthly averaged values (Hansen et al., 2005), based on SAGE II satellite data. Surface temperature is taken from GISS analysis data (Hansen et al., 2010). The global mean GISS data for AOD and temperature are interpolated in the 4.5 and 3.5 yr following the eruption, respectively. The resulting evolutions have a peak at approximately 7 and 15 months after the eruption, respectively, and then a smooth decay, which is extrapolated for 10 yr. To a 0.5 K temperature decrease at the surface, we associate a tropospheric temperature change of 0.5 K decrease below 214.4 hPa, and a 1 K increase at 87.7 hPa, following the observations from Free and Angell (2002), and interpolate between these values. These profile changes are then scaled with the magnitude of the surface temperature change. For ozone decrease, we use an evolution that has a peak of 4.5 % 2 yr after the eruption and then decays to 0, following the results of Randel et al. (1995).

The water vapour profile as a function of temperature change is evaluated using the Clausius-Clapeyron equation, assuming constant relative humidity. Variations in emissions of CH_4 from wetlands due to temperature are calculated using the Q_{10} temperature dependence relation (Dunfield et al., 1993), with a Q_{10} value of 2. For a temperature decrease of 0.5 K, we find that CH_4 wetland emissions decrease from 171.8 Tg yr^{-1} to 165.9 Tg yr^{-1} .

The second set contains two additional transient simulations, which enable us to compare the magnitude of natural effects after the eruption to that of variations in anthropogenic sources. In both simulations we employ yearly anthropogenic emissions from EDGAR 4.1, while keeping the biomass burning emissions constant at 1990 values. In the first simulation, natural emissions and atmospheric parameters are kept constant. In the second one we also include the natural forcings after the eruption. These simulations are performed starting from the steady state in the year 1890, using EDGAR-HYDE and EDGAR 4.1 emissions for the spin-up period between 1890 and 1990.

2.5 Methyl chloroform model

For validating the transient OH concentrations obtained with our column chemistry model, we perform an offline simulation of methyl chloroform (MCF) for the period 1988 to 2005. We use the same column model, with only one chemical tracer, MCF.

The MCF emissions used are the same as described in Montzka et al. (2011b). The main sink of MCF is the reaction with OH in the troposphere. We use OH fields from each time step of the transient simulation for the period 1890 to 2005

Table 3. Yearly emissions for 1890 and 1990 implemented in the model. Emission units are given in parentheses.

Species (unit)	1890	1990
CH_4 (Tg yr^{-1})	278	512
NO_x (Tg N yr^{-1})	22.7	47.6
CO (Tg yr^{-1})	460	1177
NMVOC (Tg C yr^{-1})	707	808

(the first simulation of the second set), and a temperature-dependent reaction rate as given in JPL 2011 (Sander et al., 2011). Additional stratospheric and ocean sinks are considered with lifetimes of 38 and 80 yr, respectively. These are in the range of values found by Krol and Lelieveld (2003).

We use an initial condition in 1988 of 115 ppt throughout the column.

3 Results and discussion

3.1 Model evaluation

Even though the model presented above contains many simplifications, we will show that it performs reasonably well in representing the global state of the troposphere.

Figure 2 presents the steady-state profiles for CH_4 , O_3 , NO_x , and CO obtained by the column chemistry model for the years 1890 and 1990. The yearly emission values used are shown in Table 3. CH_4 decreases with altitude by about 100 ppb throughout the troposphere in the year 1990. CO mixing ratios for the same year decrease with altitude from 125 ppb at the surface to 30 ppb near the tropopause. The NO_x profile has the typical C-shape due to the production of NO_x by lightning throughout the column and the longer lifetime of NO_x in the upper troposphere. Ozone mixing ratios decrease with altitude in the first few kilometers, and then increase towards the stratosphere.

Between the years 1890 and 1990, we find increases in ozone, CO and CH_4 , which are more pronounced near the surface due to increases in emissions of ozone precursors, CO and CH_4 . For NO_x we find increases both near the surface, because of increased emissions, as well as near the tropopause, due to an increase in the NO_x lifetime at this altitude. This is consistent with a decrease in OH in the upper troposphere due to higher CH_4 concentrations. In the study of Wang and Jacob (1998), zonal averaged profiles for ozone, OH, NO_x and CO are computed using a three-dimensional model of tropospheric chemistry for preindustrial and year 1990 conditions. Concentrations of ozone and NO_x near the surface are somewhat higher in our model, possibly due to the fact that no differentiation is made between land and ocean in our simplified single column model. Our model finds a higher CO variability throughout the column, which may be caused by the fact that we did not

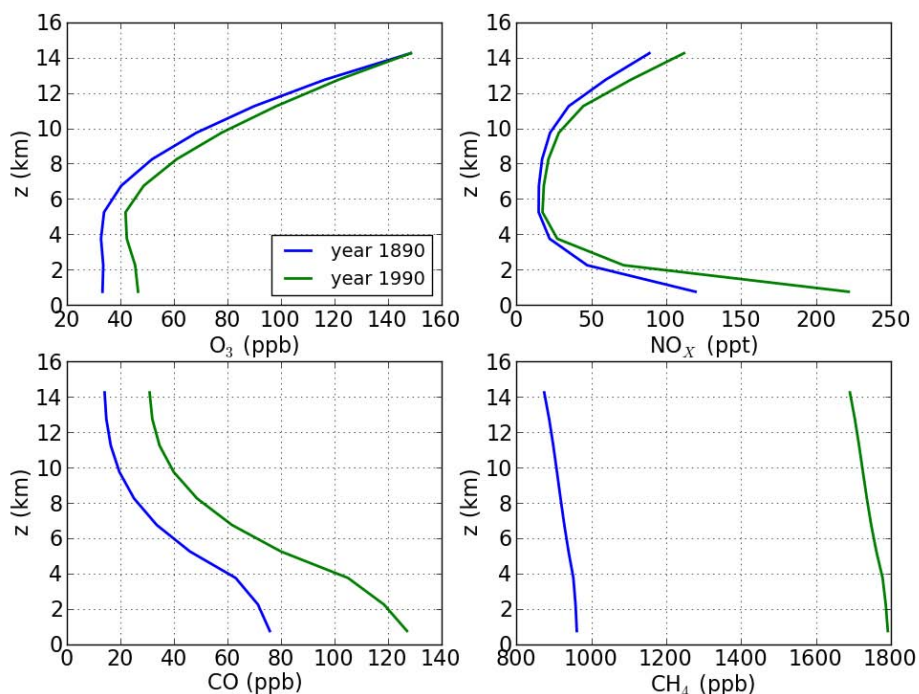


Fig. 2. Vertical profiles of ozone, NO_x , CO, and CH_4 obtained with the one dimensional model for the years 1890 and 1990.

Table 4. Comparison of trace gas budgets for the global troposphere obtained with our one-dimensional model, with the results from other models. Numbers in Tg yr^{-1} , unless otherwise specified.

	Stevenson et al. (2006), S1 scenario	Shindell et al. (2006)	Williams et al. (2012)	One-dimensional model
Ozone chemical production	5110 ± 606		4729	6117
Ozone chemical loss	4668 ± 727			5009
Ozone deposition	1003 ± 200		863	1349
Ozone stratospheric exchange	552 ± 168		274	241
Ozone burden (Tg)	344 ± 39		320	448
Ozone lifetime (days)	22.3 ± 2		23.4	25.7
OH (molec cm^{-3})		11.3 ± 1.7		9.5
OH production from photolysis			1663	2061
OH chemical production			3522	3519
CO chemical production		1505 ± 236	1314	1400
CO burden (Tg)			322	368
CO lifetime (days)			48.3	52.1
CH_4 lifetime (yrs)	8.76 ± 1.32	9.7 ± 1.7	8.35	8.2

formulate a convective redistribution of the column. In terms of changes in concentrations between the preindustrial setup and the year 1990, our model finds generally lower relative changes than the study of Wang and Jacob for O_3 , NO_x and CO, possibly due to the different emission sets that are used. However, the 30 % increase in OH that we find in the lowest 1.5 km of the model, and about 20 % decrease between 6 and 12 km altitude compare well with their study.

In Table 4, we compare the ozone, OH and CO budgets given by our model for the year 1990 to global budgets

found by several 3-dimensional chemistry transport models presented in Williams et al. (2012); Stevenson et al. (2006); Shindell et al. (2006). Overall, our model falls within the uncertainties of these models in terms of OH and CO burdens and budgets. CO and CH_4 lifetimes are also modeled realistically, certainly when one considers the huge simplifications of the chemical system and the simplified representation of the global atmosphere. Ozone burden, production, and deposition are high compared to full 3-D models. These are more representative of tropical values than global ones, likely due

to the choice of tropical conditions to represent the global troposphere. For the same reason, ozone stratospheric inflow is quite low. This is because most ozone inflow occurs in the extratropics (Gettelman et al., 2011), while our model column is in the tropics.

3.1.1 Model sensitivities

We further evaluate the sensitivity of the model to parameters involved in this study, i.e. to CH₄ and isoprene emissions, ozone column, temperature and water vapour (Table 5). We compare the sensitivities of our model to sensitivities of 2-D and 3-D models present in literature. Except for the sensitivity to CH₄ emissions, these studies evaluate other sensitivities while keeping CH₄ concentrations fixed, or by looking at timescales of a few years. Because of the CH₄ lifetime of about 8 yr, the feedback of CH₄ concentrations on its own lifetime is ineffective on such a short period. Therefore we also calculate these sensitivities while keeping CH₄ concentrations fixed.

The effect of CH₄ emission changes on the CH₄ concentrations is enhanced by the feedback via the CH₄ lifetime. To describe this process, a feedback factor a is defined as $a = 1/(1 - \frac{d \ln \tau}{d \ln \text{CH}_4})$, following Voulgarakis et al. (2012). Here τ stands for the CH₄ lifetime, and the small offsets $d \ln \text{CH}_4$ and $d \ln \tau$ are determined by a small perturbation in CH₄ emissions. We find that a has a value of 1.45 for the year 1990, which compares well with the best estimate of the Third Assessment Report of the IPCC (Prather et al., 2001), and falls well in the range found in the model intercomparison study of Voulgarakis et al. (2012).

Another sensitivity that is important to our study is the sensitivity of CH₄ to changes in the ozone column. In the two-dimensional modelling study of Bekki and Pyle (1994), a 6 % increase in OH is found due to a 6 % decrease in stratospheric ozone between the years 1991 and 1993. We find that a 6 % decrease in ozone column leads to a 6.4 % enhancement in OH, which compares well to their results. Other studies that assess the sensitivity of CH₄ and OH to ozone column changes find lower sensitivities (Camp et al., 2001; Fuglestedt et al., 1994). However, the ozone perturbations in these studies are dominated by the middle and high latitudes, where ozone photolysis and CH₄ oxidation are less important. After the Pinatubo eruption, both low and high latitude ozone columns were affected (Chipperfield et al., 2003). Therefore we consider it more appropriate to compare our results to Bekki and Pyle (1994).

To test the sensitivity of our model to climate, we used a temperature increase of 1 K throughout the column, and computed the corresponding change in humidity using the Clausius-Clapeyron equation. The CH₄ lifetime change of -0.49 yr K^{-1} in our model is somewhat larger than the multimodel mean of $-0.31 \pm 0.14 \text{ yr K}^{-1}$ found in Voulgarakis et al. (2012). However, we do not include changes in stratospheric ozone related to temperature. We use observed

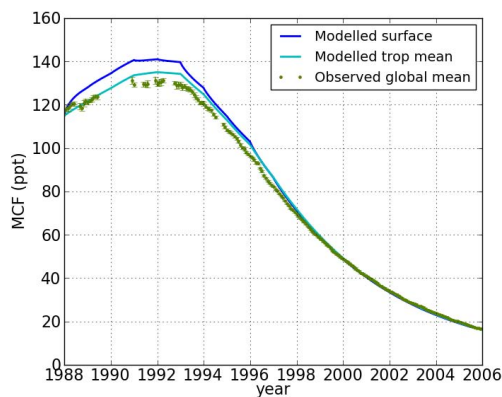


Fig. 3. Observed and modeled evolution of methyl chloroform surface and tropospheric mean mixing ratios between 1988 and 2006.

changes in stratospheric ozone, and the effect of temperature on ozone concentrations is included in the observations. The two models used in Voulgarakis et al. (2012) that also do not include this feedback give higher sensitivities to temperature, of -0.4 and -0.57 yr K^{-1} . Therefore we consider our model to respond to temperature changes in a similar manner as global chemistry models.

Telford et al. (2010) found a maximum decrease in isoprene emissions of 9 % due to lower temperature and lower PAR fluxes in the year 1992 due to the presence of aerosols in the stratosphere. They find a corresponding 1 % increase in OH tropospheric burden. We test the sensitivity of our model to such a perturbation in isoprene emissions, and find that our model is two times more sensitive. We attribute this again to our one-column approach, in which we cannot account for horizontal transport. Isoprene reacts rapidly with OH, and regions with large and small isoprene emissions are present in the true atmosphere. Furthermore, our simplified chemistry scheme is not well suited to explore the sensitivity to changing NMVOC emissions. A more recent study shows that the effect of aerosols on isoprene emissions is smaller if diffuse and direct radiation is treated separately (Wilton et al., 2011). We conclude therefore that the calculated feedback of NMVOC emissions on OH is highly uncertain, and we decide not to include it in further simulations. We simply note that decreases (increases) in NMVOC emissions probably lead to more (less) OH and a shorter (higher) CH₄ lifetime.

3.1.2 Evaluation of CH₄ and methyl chloroform concentrations

The results on MCF surface and tropospheric mean mixing ratios are shown in Fig. 3. We compare our simulation results to the observations-based global mean mixing ratios, computed by averaging the GAGE/AGAGE data at the stations Mace Head, California, Barbados, Samoa, and Cape Grim.

Table 5. Sensitivities and feedback factors of our column chemistry model and comparison to literature.

Sensitivity	1-D model	Value in literature	Study
Feedback factor between CH ₄ emissions and CH ₄ concentrations	1.45	1.4 1.23–1.69	IPCC TAR, Prather et al. (2001) Voulgarakis et al. (2012)
Change in tropospheric OH due to a 6 % increase in ozone column (%)	6.4	6	Bekki and Pyle (1994)
Change in CH ₄ lifetime due to a 1 K increase in global temperature (yr K ⁻¹)	-0.49	-0.31 ± 0.14	Voulgarakis et al. (2012)
Change in tropospheric OH due to a 9 % decrease in isoprene emissions (%)	1.9	1.	Telford et al. (2010)

The modelled total lifetime of MCF is 4.6 yr and the lifetime with respect to OH is 5.7 yr, in agreement with other studies (Krol and Lelieveld, 2003; Prinn et al., 2005). When we sample the model at the surface in the period in which MCF emissions were significant (1988–1998), the model is seen to overestimate the observed mixing ratios. This is related to differences in the sampling of the model and the observations. Observations are generally taken in remote areas, away from the emissions, in order to be representative for the global burden. In our one-dimensional model, the sampling is done in the surface grid box, where the emissions are also put in. Therefore a tropospheric mean sampling of the model is in better correspondence with the observations. This is confirmed by the fact that our modelled tropospheric mean MCF mixing ratios are in very good agreement with GAGE/AGAGE observations. A tropospheric mean sampling of the model will be used in the rest of the paper.

The results for CH₄ concentrations from the first simulation of the second set, as defined in Sect. 2.4, are shown in Fig. 4. They are compared to global means for the period 1890 to 1990, calculated from ice core measurements in Etheridge et al. (1998). Following the same procedure as used in Etheridge et al. (1998), we estimate global mean mixing ratios for the period 1985 to 2005 based on the monthly means from the GLOBALVIEW-CH₄ (2009) data from the stations Alert and South Pole. The global mean is therefore computed as the mixing ratio at South Pole plus 37 % of the interpolator difference. Modelled CH₄ mixing ratios generally follow the decadal trends in CH₄ emissions, with a delay of about 10 yr due to the CH₄ lifetime. The stabilization of the concentrations towards the end of the simulation period is a phenomenon that is also present in the observations (Dlugokencky et al., 2003).

Compared to the observations, our model follows quite well the trends in CH₄ mixing ratios, but generally overestimates CH₄ mixing ratios by up to 50 ppb. We expect this to happen in the first decades of the simulation, because the starting point represents a steady state, while the system might not have been in equilibrium in the year 1890. The concentration continues to be overestimated until 1990, pointing either to an overestimation of the CH₄ emissions

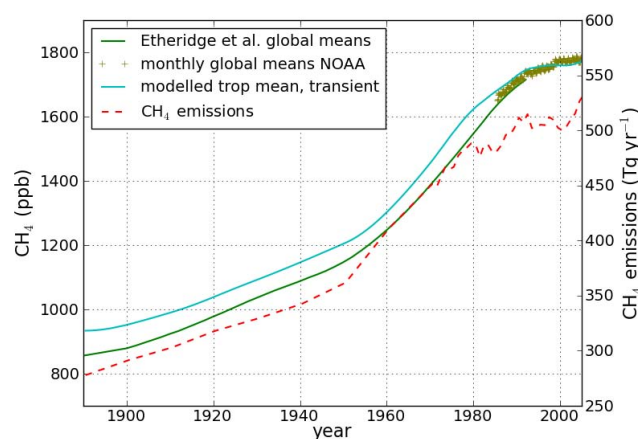


Fig. 4. Observed and modeled evolution of CH₄ mixing ratios between 1890 and 2005. Observation-based global means are calculated by Etheridge et al. (1998) based on ice-core data (green line), and more recent global means are calculated using measurements at South Pole and Alert NOAA stations (green crosses). CH₄ emissions implemented in the model are also shown (red dotted line, with scale on the right axis) (Van Aardenne et al., 2001; Spahni et al., 2011).

or of the CH₄ lifetime in this period. These results are only based on changing anthropogenic emissions (NO_x, CO, CH₄, NMVOC) for the simulated period, and there are several possible explanations for the differences between modelled and observed concentrations. Firstly, processes not included here, such as changes in stratospheric ozone, temperatures and possible trends in natural and biomass burning emissions can have a significant impact on CH₄ concentrations. Secondly, we are not able to represent high and low NO_x regions in our column chemistry model. For this reason, our model might misrepresent the sensitivity of CH₄ concentrations to NO_x and NMVOC emissions. Finally, we use a fixed CO yield from NMVOC oxidation for the simulated period. This yield varies among species and among NO_x pollution environments, therefore we would expect it to change on a centennial scale. However, the chosen model setup captures the observed range of CH₄ concentrations in the period 1990–2005, which is the period we are interested in.

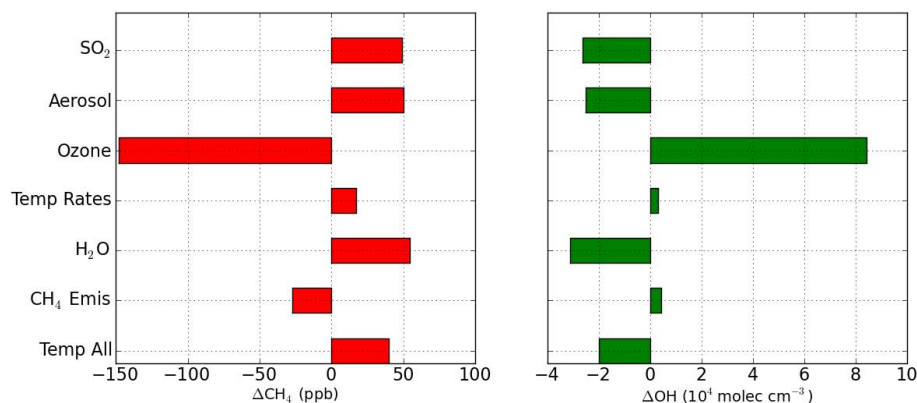


Fig. 5. CH₄ and OH steady-state changes due to various Pinatubo forcings.

We conclude that our model properly represents the global budgets and lifetimes of the different species, and is able to reproduce the mean state of the atmosphere in the 1990s. The sensitivities relevant for this study are reasonably represented. However, the model is too simplified to capture variations of CH₄ on a centennial scale, or vertical profiles of different species present in the model. Our sensitivity tests also show that the sensitivity of the model to NMVOC emissions is overestimated.

3.2 The Pinatubo eruption

3.2.1 Steady-state perturbations

We first examine the effect of each of the forcings of the Pinatubo eruption described in Table 2 on the CH₄ equilibrium concentration, using the maximum magnitude of each forcing. The differences in tropospheric CH₄ and OH between each simulation and the “base” simulation are shown in Fig. 5.

We find that the 5 % reduction in ozone column has the largest effect on the tropospheric mean CH₄ equilibrium mixing ratio, decreasing it by 125 ppb. SO₂, aerosol and water vapour changes all increase the CH₄ steady-state by 48 to 55 ppb. The effects of temperature decrease on CH₄ emissions and reaction rates have smaller impacts on the simulated steady-state mixing ratios, of 27 and 17 ppb respectively. The temperature-related processes, that is “Temp Rates”, “H₂O” and “CH₄ Emis”, partly cancel each other, resulting in an overall increase of 40 ppb.

Except for the effects of changed CH₄ emissions and changed reaction rates, the effects on CH₄ are strongly correlated to effects on OH of the same relative magnitude and of opposite sign. The OH response to decreasing CH₄ emissions reflects the effectiveness of the feedback factor introduced in the previous section. Changed reaction rates due to tropospheric cooling lead to a small increase in OH, because of the slower oxidation rate of CH₄.

3.2.2 Evolution of transient concentrations and growth rate

The modelled transient evolution of CH₄ mixing ratios due to individual natural perturbations following the eruption, and including their overall effect, are shown in Fig. 6a. When all natural effects are included, the tropospheric mean CH₄ mixing ratio slightly increases for 9 months after the eruption. Afterwards it decreases, reaching a maximum decrease of 13 ppb about 6 yr after the eruption. The magnitudes of the perturbations in transient concentrations are smaller than the effects on the steady states, occurring at different moments in time after the eruption and on different timescales. Because the CH₄ lifetime is about 8 yr, the concentration at one moment in time shows an integrated effect of its source-sink imbalance in the previous years. Therefore not only the magnitude, but also the duration of the perturbation plays an important role in determining its effect on CH₄ concentrations. The recovery time to the initial concentration is much longer compared to the recovery time of the perturbations applied. The SO₂ effect is hardly observed in the transient concentrations, because of its short duration. All the other processes affect the CH₄ concentration for up to 40 yr after the eruption.

We calculate the CH₄ growth rate by differentiating the transient mixing ratios. The overall effect of the natural forcings after Pinatubo on the tropospheric CH₄ growth rate (Fig. 6b) is a positive jump of 3 ppb yr⁻¹ due to UV absorption by SO₂ immediately after the eruption. The effect decreases, but remains positive for about 9 months after the eruption, due to the presence of SO₂ and sulphate aerosols in the stratosphere. After that, the effect on the CH₄ growth rate is dominated by the forcing exerted by ozone depletion, partly counteracted by decreased water vapour. The overall effect of natural forcings on CH₄ growth rate experiences a minimum of -5 ppb yr⁻¹ about 2 yr after the eruption. The growth rate increases afterwards, reaching zero about 6 yr after the eruption, when the effect on the transient CH₄ mixing ratios is at a minimum (Fig. 6a). The slow recovery of the

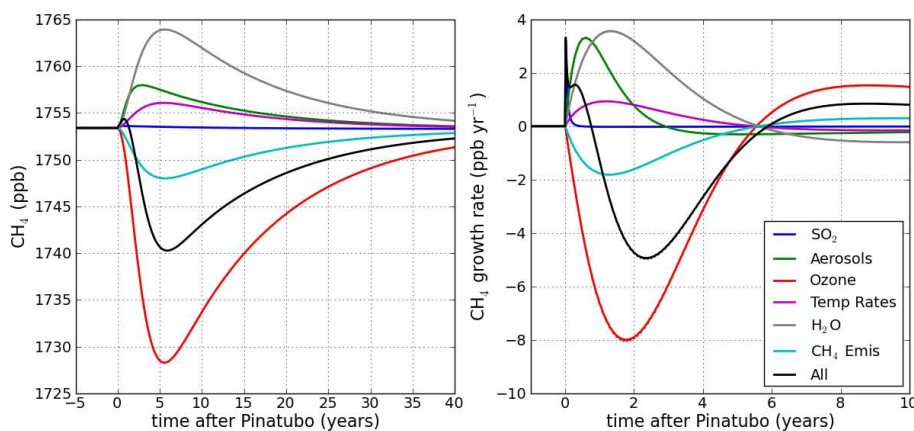


Fig. 6. Effect of the different Pinatubo forcings on the temporal evolution of the tropospheric mean CH_4 mixing ratio and growth rate.

concentrations to the steady state is marked by a small positive growth rate of less than 1 ppb yr^{-1} . The shape of the growth rate evolution reflects the annual imbalance between CH_4 sources and sinks.

We find a positive CH_4 growth rate for about 9 months after the eruption. The effect of temperature on the reaction rates is small in this period, and the temperature effect on emissions leads to a negative growth rate. Therefore we can only relate this positive growth rate to a decrease in OH, as also suggested by Dlugokencky et al. (1996). The large effect of ozone depletion which follows compares well with the results of Bekki et al. (1994). They report a 7 ppb yr^{-1} decrease in growth rate from spring 1991 to autumn 1992 due to ozone depletion. The drop in CH_4 growth rate due to ozone depletion in our model is associated with a 5% increase in OH. This is consistent with the findings of Wang et al. (2004) of a global drop in OH of $10^5 \text{ molec cm}^{-3}$, equivalent to 7%, between the end of 1991 and beginning of 1994. Using the same parametric model, but keeping stratospheric ozone constant, they find much smaller variability in OH in this period, on the order of 1–2%. Similar to our results, Bousquet et al. (2006) find an increase in the OH sink until the beginning of 1992, and then a subsequent decrease in 1992 and 1993. However, they find different magnitudes of these changes compared to our study, leading to an overall increase in the OH sink between 1991 and 1993. The magnitude of the temperature-related effects that we find compares well with the estimate from Bekki and Law (1997). We find a maximum of 6 Tg yr^{-1} change in wetland emissions after the eruption. This is similar to the bottom up estimate of about 5 Tg yr^{-1} shown in Spahni et al. (2011) Fig. 8a, but a few times lower than the maximum anomaly of about 40 Tg yr^{-1} found in the inverse modelling study of Bousquet et al. (2006). Our lower estimate might be partly due to the fact that we considered changes in CH_4 emissions solely due to temperature. CH_4 emissions also depend on spatial and temporal changes in soil moisture and precipitation, which have been observed after the eruption (Spahni et al., 2011).

Changes in wetland extent were also shown to have a large impact on the interannual variability in CH_4 emissions from wetlands (Ringeval et al., 2010), which is also not taken into account in the study of Spahni et al. (2011) for the years 1991 and 1992. In addition, we consider a global Q_{10} factor of 2, while this factor was shown to be dependent on ecosystem type, with a range of measured values between 1.6 and 16 (Dunfield et al., 1993; Valentine et al., 1994).

The results show that stratospheric ozone changes had a large impact on CH_4 growth rate after the eruption. The WMO 2003 report (Chipperfield et al., 2003) shows that the total ozone in the atmosphere decreased between the years 1991 and 1993 by about 5%. Similar numbers are found when excluding the high latitudes (for $60^\circ \text{ S}–60^\circ \text{ N}$), or when looking only at the tropical region ($25^\circ \text{ S}–25^\circ \text{ N}$). This change was caused partly by natural variability, including an increase in the solar activity in this period, and partly by processes related to the eruption. Therefore, after removing the effects of the solar cycle and QBO, a decrease of 2% to 3% is found in the measured total ozone between 1991 and 1993. CH_4 measurements are affected by changes in the ozone column, irrespective of their cause. For this reason, we used here a maximum decrease of 4.5% in the ozone column, representative for $60^\circ \text{ S}–60^\circ \text{ N}$, which includes solar variability. To distinguish the change in CH_4 concentrations due to changes in ozone related to the eruption, a smaller perturbation should be considered.

The modelled CH_4 growth rate from the second set of simulations, when varying anthropogenic emissions of CH_4 , CO , NO_x and NMVOC, is shown in Fig. 7. These simulations have a starting point in 1890, producing a more realistic growth rate at the moment of the eruption of 10 ppb yr^{-1} . Results for the full length of the simulation, without including the post-Pinatubo perturbations, are shown in Fig. 4. We compare our results with the observations-based global mean growth rate, obtained by globally averaging the CH_4 reference marine boundary layer matrix from GLOBALVIEW- CH_4 (2009), and deseasonalising it using

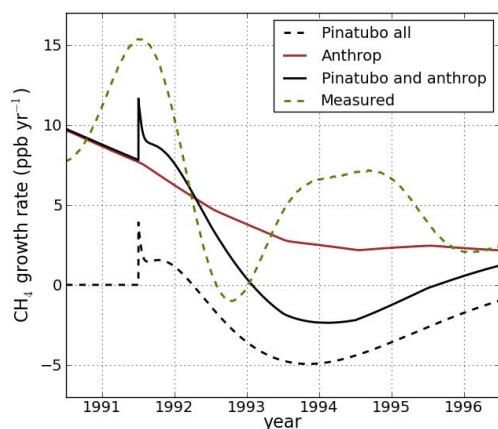


Fig. 7. Modelled growth rate evolution after the Pinatubo eruption including variations due to anthropogenic emissions, and the combined signal from natural and anthropogenic changes. The black dotted line shows the growth rate evolution obtained in the first set of simulations, including all natural forcings (the same as the black line in Fig. 6b). Also shown is the measured globally averaged growth rate obtained using the reference marine boundary layer matrix from GLOBALVIEW-CH₄ (2009).

the software provided by NOAA (based on Thoning and Tans (1989)). CH₄ anthropogenic emissions were relatively stable in the years 1990 to 2000, while anthropogenic NO_x emissions increased and CO emissions decreased. Therefore we find a generally decreasing trend in CH₄ growth rate due to a decrease in CH₄ lifetime, when only variations in anthropogenic emissions are taken into account.

When both variations in anthropogenic emissions and natural forcings are included in the model, a similar range of values is found for the modelled and observed growth rates in the years 1991 to 1996. These values vary between more than 10 ppb yr⁻¹ and slightly negative values of up to -2 ppb yr⁻¹. Decreased anthropogenic CH₄ emissions between the years 1991 and 1993 are found to contribute by an additional 5 ppb yr⁻¹ to the drop in CH₄ growth rate in this period, in agreement with previous studies (Dlugokencky et al., 1994; Bousquet et al., 2006). The timing of the minimum growth rate after the eruption is modelled about 15 months later than that observed. This minimum is found by a complex balance between the different forcings, being later than the minimum in any of the individual forcings applied. Therefore the discrepancy between the timing of the modelled minimum and of the observed one might be related to the simplified evolution of the temperature and ozone changes applied, or the fact that some sources of variability (see below) are not taken into account. This might also explain the fact that the increased growth rate in 1994 is not captured in our simplified simulations.

By comparing the sum of the “Pinatubo all” and “Anthrop” curves to the growth rate evolution when including both Pinatubo forcings and changes in anthropogenic emissions, we find that the effect of nonlinearity on growth rates is less than 10%.

Since our study is an idealised sensitivity study, there are many possible reasons for differences between the modelled and the observed growth rate. Firstly, many processes known to determine CH₄ variability are not included here. These include changes in biomass burning emissions (Bousquet et al., 2006), isoprene emissions (Telford et al., 2010) and variability in wetland emissions due to atmospheric changes related to the El Niño Southern Oscillation (ENSO) cycle (Hodson et al., 2011). Secondly, differences may result from the different sampling of the model and the observations, as already mentioned in Sect. 3.1.2. The interpolation procedure used to obtain the observed global CH₄ growth rate curve can also smoothen out some sudden variations in the CH₄ growth rate, such as the jump due to the SO₂ injected by the eruption. Finally, there are uncertainties related to our model setup, on which we elaborate further below.

In order to show that our results are robust with respect to the parameters used in the model, a series of sensitivity tests was performed. We tested different temperature and water vapour profiles, a higher value for the CO yield from the oxidation of NMVOC, including NMVOC recycling, and increased vertical mixing. Although the effect on the modelled CH₄ concentrations in the last century may be on the order of 100 ppb (results not shown), the effect on the growth rate evolution after the eruption is less than 10%. Changing the temperature by -2.5 K to +1 K and simultaneously changing the water vapour profile according to the Clausius-Clapeyron equation lead to changes in the CH₄ growth rate results of less than 0.1 ppb yr⁻¹. Similar results are obtained when changing the CO yield from NMVOC to 0.5 instead of 0.35, or when doubling the vertical mixing coefficients. Including a 0.25 yield of HO₂ from the oxidation of NMVOC in the presence of NO_x leads to a higher growth rate minimum after the eruption by 0.3 ppb yr⁻¹. We estimate therefore a maximum error of 10% in the modelled growth rate due to uncertainties in the model parameters.

Horizontal distributions of the modelled forcings can play an important role for the overall effect on the CH₄ growth rate, and cannot be simulated in our column model. This may cause additional uncertainties in our results. For example, we expect to overestimate the effect of SO₂, by inferring an instant homogenisation of the emissions. In reality, high concentrations were found close to the emission point after the eruption, and the short lifetime of SO₂ limited this effect to low latitudes (Guo et al., 2004a). Changes in stratospheric aerosol, ozone and temperature have been observed globally, but with different magnitudes at different latitudes. Since CH₄ oxidation is more important in the tropics, processes that are relatively stronger in the tropics will have a higher impact on the CH₄ lifetime.

4 Conclusions

We have implemented a column chemistry model, and tested its performance in representing the mean state of the atmosphere. Although we acknowledge that our model is simplified and difficult to apply in a globally-averaged fashion, it allowed us to quantify for the first time the combined effect of radiation and temperature-related effects after the Pinatubo eruption on the CH₄ growth rate, including feedbacks on the CH₄ lifetime. The results show that full recovery of transient CH₄ concentrations from these perturbations takes about 40 yr.

Using this simple approach, we are able to explain a large part of the observed drop in CH₄ growth rate after the eruption of Pinatubo. We conclude that a multitude of emission and lifetime effects contributed to the observed growth rate variations following the eruption, as has been suggested by previous inverse modelling studies (Bousquet et al., 2006; Wang et al., 2004). We find that about 7 ppb yr⁻¹ of the observed 17 ppb yr⁻¹ can be explained by natural processes after the eruption. The dominating effects operate through tropospheric photolysis rates, with an important contribution from ozone depletion. This shows the importance of stratospheric-tropospheric couplings, and that a good representation of stratospheric chemistry is needed in order to model accurately CH₄ concentrations. We also find that the decrease in anthropogenic emissions between 1991 and 1993 contributed by 5 ppb yr⁻¹ to the decreased CH₄ growth rate in 1993. The remaining 5 ppb yr⁻¹ of the observed drop in CH₄ growth rate remains unexplained, and might be related to changes in emissions from biomass burning or changes in biogenic NMVOC emissions.

Our model has the advantage of simplicity; however, there are processes that cannot be represented, such as horizontal transport and changes in the dynamics of the atmosphere. Additionally, we did not consider the spatial distribution of CH₄ emissions. Using a global vegetation model would allow better estimates of the response of natural emissions to changes in temperature, precipitation and radiation. Therefore, a three dimensional chemistry transport model coupled with a climate model will be used to perform future experiments.

Acknowledgements. This work was supported by the Netherlands Organisation for Scientific Research (NWO) and the EU FP7 Integrated Project PEGASOS. We thank the NOAA global air sampling network for their efforts in gathering the CH₄ measurements and the GLOBALVIEW CH₄ project for extending and integrating the data. We thank the GAGE and AGAGE networks for providing the MCF measurements used in this study.

Edited by: M. Heimann

References

- Bekki, S. and Law, K. S.: Sensitivity of the atmospheric CH₄ growth rate to global temperature changes observed from 1980 to 1992, *Tellus*, 49B, 409–416, 1997.
- Bekki, S. and Pyle, J. A.: A two-dimensional modeling study of the volcanic eruption of Mount Pinatubo, *J. Geophys. Res.*, 99, 18861–18869, 1994.
- Bekki, S., Law, K. S., and Pyle, J. A.: Effect of ozone depletion on atmospheric CH₄ and CO concentrations, *Nature*, 371, 595–597, 1994.
- Bender, F. A., Ekman, A. M. L., and Rodhe, H.: Response to the eruption of Mount Pinatubo in relation to climate sensitivity in the CMIP3 models, *Clim. Dynam.*, 35, 875–886, doi:10.1007/s00382-010-0777-3, 2010.
- Bousquet, P., Ciais, P., Miller, J. B., Dlugokencky, E. J., Hauglustaine, D. A., Prigent, C., Van der Werf, G. R., Peylin, P., Brunke, E.-G., Carouge, C., Langenfelds, R. L., Lathière, J., Papa, F., Ramonet, M., Schmidt, M., Steele, L. P., Tyler, S. C., and White, J.: Contribution of anthropogenic and natural sources to atmospheric methane variability, *Nature*, 443, 439–443, doi:10.1038/nature05132, 2006.
- Butler, T. M., Simmonds, I., and Rayner, P. J.: Mass balance inverse modelling of methane in the 1990s using a Chemistry Transport Model, *Atmos. Chem. Phys.*, 4, 2561–2580, doi:10.5194/acp-4-2561-2004, 2004.
- Camp, C. D., Roulston, M. S., Haldemann, A. F., and Yung, Y. L.: The sensitivity of tropospheric methane to the interannual variability in stratospheric ozone, *Chemosphere – Global Change Sci.*, 3, 147–156, doi:10.1016/S1465-9972(00)00053-2, 2001.
- Chipperfield, M. P., Randel, W. J., Bodeker, G. E., Dameris, M., Fioletov, V. E., Friedl, R. R., Harris, N. R. P., Logan, J. A., McPeters, R. D., Muthama, N. J., Peter, T., Shepherd, T. G., Shine, K. P., Solomon, S., Thomason, L. W., and Zawodny, J. M.: Global Ozone: Past and Future, in: *Scientific Assessment of Ozone Depletion: 2002*, Global Ozone Research and Monitoring Project, Report No. 47, chap. 4, Geneva, 2003.
- Dee, D. P., Uppala, S. M., Simmons, A. J., Berrisford, P., Poli, P., Kobayashi, S., Andrae, U., Balmaseda, M. A., Balsamo, G., Bauer, P., Bechtold, P., Beljaars, A. C. M., Berg, L. V. D., Bidlot, J., Bormann, N., Delsol, C., Dragani, R., Fuentes, M., Geer, A. J., Haimberger, L., Healy, S. B., Hersbach, H., Holm, E. V., Isaksen, L., and Kallberg, P.: The ERA-Interim reanalysis: configuration and performance of the data assimilation system, *Q. J. Roy. Meteorol. Soc.*, 137, 553–597, doi:10.1002/qj.828, 2011.
- Dlugokencky, E. J., Masarie, K. A., Lang, P. M., Tans, P. P., Steele, L. P., and Nisbet, E. G.: A dramatic decrease in the growth rate of atmospheric methane in the northern hemisphere during 1992, *Geophys. Res. Lett.*, 21, 45–48, 1994.
- Dlugokencky, E. J., Dutton, E. G., Novelli, P. C., Tans, P. P., Masarie, K. A., Lantz, K. O., and Madronich, S.: Changes in CH₄ and CO growth rates after the eruption of Mt. Pinatubo and their link with changes in tropical tropospheric UV flux, *Geophys. Res. Lett.*, 23, 2761–2764, 1996.
- Dlugokencky, E. J., Houweling, S., Bruhwiler, L., Masarie, K. A., Lang, P. M., Miller, J. B., and Tans, P. P.: Atmospheric methane levels off: Temporary pause or a new steady-state?, *Geophys. Res. Lett.*, 30, 1992, doi:10.1029/2003GL018126, 2003.
- Dlugokencky, E. J., Nisbet, E. G., Fisher, R., and Lowry, D.: Global atmospheric methane: budget, changes and dangers, *Phil. Trans.*

- R. Soc. A, 369, 2058–2072, doi:10.1098/rsta.2010.0341, 2011.
- Dunfield, P., Knowles, R., Dumont, R., and Moore, T. R.: Methane production and consumption in temperate and subarctic peat soils: Response to temperature and pH, *Soil Biol. Biochem.*, 25, 321–326, 1993.
- Elterman, L.: UV, Visible and IR Attenuation for Altitudes to 50 km, *Environ. Res. Pap.*, 285, AFCRL-68-0153, 1968.
- Etheridge, D. M., Steele, L. P., Francey, R. J., and Langenfelds, R. L.: Atmospheric methane between 1000 A. D. and present: Evidence of anthropogenic emissions and climatic variability, *J. Geophys. Res.*, 103, 15979–15993, 1998.
- European Commission and Joint Research Centre (JRC)/Netherlands Environmental Assessment Agency (PBL): Emission Database for Global Atmospheric Research (EDGAR), release version 4.1, available at: <http://edgar.jrc.ec.europa.eu/> (last access: 17 November 2011), 2010.
- Free, M. and Angell, J. K.: Effect of volcanoes on the vertical temperature profile in radiosonde data, *J. Geophys. Res.*, 107, 4101, doi:10.1029/2001JD001128, 2002.
- Fuglestedt, J. S., Johnson, J. E., and Isaksen, I. S. A.: Effects of reductions in stratospheric ozone on tropospheric chemistry through changes in photolysis rates, *Tellus*, 46B, 172–192, 1994.
- Gauci, V., Blake, S., Stevenson, D. S., and Highwood, E. J.: Halving of the northern wetland CH₄ source by a large Icelandic volcanic eruption, *J. Geophys. Res.*, 113, 1–8, doi:10.1029/2007JG000499, 2008.
- Gottelman, A., Hoor, P., Pan, L. L., Randel, W. J., Heggin, M. I., and Birner, T.: The extratropical upper troposphere and lower stratosphere, *Rev. Geophys.*, 49, RG3003, doi:10.1029/2011RG000355, 2011.
- GLOBALVIEW-CH4: Cooperative Atmospheric Data Integration Project – Methane. CD-ROM, NOAA ESRL, Boulder, Colorado, also available on Internet via anonymous FTP to <ftp://ftp.cmdl.noaa.gov/Path:ceg/ch4/GLOBALVIEW> (last access: 16 February 2012), 2009.
- Grant, A., Archibald, A. T., Cooke, M. C., and Shallcross, D. E.: Modelling the oxidation of seventeen volatile organic compounds to track yields of CO and CO₂, *Atmos. Environ.*, 44, 3797–3804, doi:10.1016/j.atmosenv.2010.06.049, 2010.
- Guenther, A. B., Zimmerman, P. R., Harley, P. C., Monson, R. K., and Fall, R.: Isoprene and Monoterpene Emission Rate Variability: Model Evaluations and Sensitivity Analyses, *J. Geophys. Res.*, 98, 12609–12617, 1993.
- Guo, S., Bluth, G. J. S., Rose, W. I., Watson, I. M., and Prata, A. J.: Re-evaluation of SO₂ release of the 15 June 1991 Pinatubo eruption using ultraviolet and infrared satellite sensors, *Geochem. Geophys. Geosyst.*, 5, Q04001, doi:10.1029/2003GC000654, 2004a.
- Guo, S., Rose, W. I., Bluth, G. J. S., and Watson, I. M.: Particles in the great Pinatubo volcanic cloud of June 1991: The role of ice, *Geochem. Geophys. Geosyst.*, 5, Q05003, doi:10.1029/2003GC000655, 2004b.
- Hansen, J., Sato, M., Ruedy, R., Nazarenko, L., Lacis, A., Schmidt, G. A., Russell, G., Aleinov, I., Bauer, M., Bell, N., Cairns, B., Canuto, V., Chandler, M., Cheng, Y., Del Genio, A., Faluvegi, G., Fleming, E., Friend, A., Hall, T., Jackman, C., Kelley, M., Kiang, N., Koch, D., Lean, J., Lerner, J., Lo, K., Menon, S., Miller, R., Minnis, P., Novakov, T., Oinas, V., Perlwitz, J., Perlwitz, J., Rind, D., Romanou, A., Shindell, D., Stone, P., Sun, S., Tausnev, N., Thresher, D., Wielicki, B., Wong, T., Yao, M., and Zhang, S.: Efficacy of climate forcings, *J. Geophys. Res.*, 110, D18104, doi:10.1029/2005JD005776, 2005.
- Hansen, J., Ruedy, R., Sato, M., and Lo, K.: Global surface temperature change, *Rev. Geophys.*, 48, RG4004, doi:10.1029/2010RG000345, 2010.
- Hodson, E. L., Poulter, B., Zimmermann, N. E., Prigent, C., and Kaplan, J. O.: The El Niño Southern Oscillation and wetland methane interannual variability, *Geophys. Res. Lett.*, 38, 3–6, doi:10.1029/2011GL046861, 2011.
- Huijnen, V., Williams, J., van Weele, M., van Noije, T., Krol, M., Dentener, F., Segers, A., Houweling, S., Peters, W., de Laat, J., Boersma, F., Bergamaschi, P., van Velthoven, P., Le Sager, P., Eskes, H., Alkemade, F., Scheele, R., Nédélec, P., and Pätz, H.-W.: The global chemistry transport model TM5: description and evaluation of the tropospheric chemistry version 3.0, *Geosci. Model Develop.*, 3, 445–473, doi:10.5194/gmd-3-445-2010, 2010.
- Kinnison, D. E., Grant, K. E., Connell, P. S., Rotman, D. A., and Wuebbles, D. J.: The chemical and radiative effects of the Mount Pinatubo eruption, *J. Geophys. Res.*, 99, 25,705–25,731, 1994.
- Krol, M. and Lelieveld, J.: Can the variability in tropospheric OH be deduced from measurements of 1,1,1-trichloroethane (methyl chloroform)?, *J. Geophys. Res.*, 108, 4125, doi:10.1029/2002JD002423, 2003.
- Lowe, D. C., Manning, M. R., Brailsford, G. W., and Bromley, A. M.: The 1991–1992 atmospheric methane anomaly: Southern hemisphere 13C decrease and growth rate fluctuations, *Geophys. Res. Lett.*, 24, 857–860, doi:10.1029/97GL00830, 1997.
- Madronich, S.: UV radiation in the natural and perturbed atmosphere, in: *Environmental effects of UV (Ultraviolet) radiation*, edited by Tevini, M., 17–69, Lewis Publisher, Boca Raton, FL, USA, 1993.
- McCormick, M. P., Thomason, L. W., and Trepte, C. R.: Atmospheric effects of the Mt. Pinatubo eruption, *Nature*, 373, 399–404, 1995.
- Monteil, G., Houweling, S., Dlugokencky, E. J., Maenhout, G., Vaughn, B. H., White, J. W. C., and Rockmann, T.: Interpreting methane variations in the past two decades using measurements of CH₄ mixing ratio and isotopic composition, *Atmos. Chem. Phys.*, 11, 9141–9153, doi:10.5194/acp-11-9141-2011, 2011.
- Montzka, S. A., Dlugokencky, E. J., and Butler, J. H.: Non-CO₂ greenhouse gases and climate change, *Nature*, 476, 43–50, doi:10.1038/nature10322, 2011a.
- Montzka, S. A., Krol, M., Dlugokencky, E., Hall, B., Jockel, P., and Lelieveld, J.: Small Interannual Variability of Global Atmospheric Hydroxyl, *Science*, 331, 67–69, doi:10.1126/science.1197640, 2011b.
- Niemeier, U., Timmreck, C., Graf, H.-F., Kinne, S., Rast, S., and Self, S.: Initial fate of fine ash and sulfur from large volcanic eruptions, *Atmos. Chem. Phys.*, 9, 9043–9057, doi:10.5194/acp-9-9043-2009, 2009.
- Prather, M., Ehhalt, D., Dentener, F., Derwent, R., Dlugokencky, E., Holland, E., Isaksen, I. S. A., Katima, J., Kirchhoff, V., Matson, P., Midgley, P. M., and Wang, M.: Atmospheric Chemistry and Greenhouse Gases, in: *Climate Change 2001: The Scientific Basis, Contribution of Working Group I to the Third Assessment Report of the Intergovernmental Panel on Climate Change*, 239–288, Cambridge Univ. Press, New York, USA, 2001.

- Prinn, R. G., Huang, J., Weiss, R. F., Cunnold, D. M., Fraser, P. J., Simmonds, P. G., McCulloch, A., Harth, C., Reimann, S., Salameh, P., O'Doherty, S., Wang, R. H. J., Porter, L. W., Miller, B. R., and Krummel, P. B.: Evidence for variability of atmospheric hydroxyl radicals over the past quarter century, *Geophys. Res. Lett.*, 32, L07809, doi:10.1029/2004GL022228, 2005.
- Quay, P., Stutsman, J., Wilbur, D., Snover, A., Dlugokencky, E., and Brown, T.: The isotopic composition of atmospheric methane, *Global Biogeochem. Cy.*, 13, 445–461, doi:10.1029/1998GB900006, 1999.
- Randel, J. W., Wu, F., Russell III, J., Waters, J., and Froidevaux, L.: Ozone and temperature changes in the stratosphere following the eruption of Mount Pinatubo, *Geophys. Res. Lett.*, 100, 16753–16764, 1995.
- Ringeval, B., de Noblet-Ducoudré, N., Ciais, P., Bousquet, P., Prigent, C., Papa, F., and Rossow, W. B.: An attempt to quantify the impact of changes in wetland extent on methane emissions on the seasonal and interannual time scales, *Global Biogeochem. Cy.*, 24, GB2003, doi:10.1029/2008GB003354, 2010.
- Russell, P. B., Livingston, J. M., Poeschel, R. F., Bauman, J. J., Pollack, J. B., Brooks, S. L., Hamill, P., Thomason, L. W., Stowe, L. L., Deshler, T., Dutton, E. G., and Bergstrom, R. W.: Global to microscale evolution of the Pinatubo volcanic aerosol derived from diverse measurements and analyses, *J. Geophys. Res.*, 101, 18745–18763, 1996.
- Sander, S. P., Friedl, R. R., Barker, J. R., Golden, D. M., Kurylo, M. J., Wine, P. H., Abbatt, J. P. D., Burkholder, J. B., Kolb, C. E., Moortgat, G. K., Huie, R. E., and Orkin, V. L.: Chemical Kinetics and Photochemical Data for Use in Atmospheric Studies, Tech. Rep. 17, Jet Propulsion Laboratory, NASA, Pasadena, California, USA, 2011.
- Schauffler, S. M. and Daniel, J. S.: On the effects of stratospheric circulation changes on trace gas trends, *J. Geophys. Res.*, 99, 25747–25754, 1994.
- Shindell, D. T., Faluvegi, G., Stevenson, D. S., Krol, M. C., Emmons, L. K., Lamarque, J.-F., Pétron, G., Dentener, F. J., Ellingsen, K., Schultz, M. G., Wild, O., Amann, M., Atherton, C. S., Bergmann, D. J., Bey, I., Butler, T., Cofala, J., Collins, W. J., Derwent, R. G., Doherty, R. M., Drevet, J., Eskes, H. J., Fiore, A. M., Gauss, M., Hauglustaine, D. A., Horowitz, L. W., Isaksen, I. S. A., Lawrence, M. G., Montanaro, V., Müller, J.-F., Pitari, G., Prather, M. J., Pyle, J. A., Rast, S., Rodriguez, J. M., Sanderson, M. G., Savage, N. H., Strahan, S. E., Sudo, K., Szopa, S., Unger, N., van Noije, T. P. C., and Zeng, G.: Multimodel simulations of carbon monoxide: Comparison with observations and projected near-future changes, *J. Geophys. Res.*, 111, D19306, doi:10.1029/2006JD007100, 2006.
- Soden, B. J., Wetherald, R. T., Stenchikov, G. L., and Robock, A.: Global Cooling After the Eruption of Mount Pinatubo: A Test of Climate Feedback by Water Vapor, *Science*, 296, doi:10.1126/science.296.5568.727, 2002.
- Spahn, R., Wania, R., Neef, L., van Weele, M., Pison, I., Bousquet, P., Frankenberg, C., Foster, P. N., Joos, F., Prentice, I. C., and van Velthoven, P.: Constraining global methane emissions and uptake by ecosystems, *Biogeosciences*, 8, 1643–1665, doi:10.5194/bg-8-1643-2011, 2011.
- Stevenson, D. S., Dentener, F. J., Schultz, M. G., Ellingsen, K., van Noije, T. P. C., Wild, O., Zeng, G., Amann, M., Atherton, C. S., Bell, N., Bergmann, D. J., Bey, I., Butler, T., Cofala, J., Collins, W. J., Derwent, R. G., Doherty, R. M., Drevet, J., Eskes, H. J., Fiore, A. M., Gauss, M., Hauglustaine, D. A., Horowitz, L. W., Isaksen, I. S. A., Lawrence, M. G., Montanaro, V., Müller, J.-F., Pitari, G., Prather, M. J., Pyle, J. A., Rast, S., Rodriguez, J. M., Sanderson, M. G., Savage, N. H., Strahan, S. E., Sudo, K., Szopa, S., Unger, N., van Noije, T. P. C., and Zeng, G.: Multimodel ensemble simulations of present-day and near-future tropospheric ozone, *J. Geophys. Res.*, 111, D08301, doi:10.1029/2005JD006338, 2006.
- Telford, P. J., Lathiere, J., Abraham, N. L., Archibald, A. T., Braesicke, P., Johnson, C. E., Morgenstern, O., O'Connor, F. M., Pike, R. C., Wild, O., Young, P. J., Hewitt, C. N., and Pyle, J.: Effects of climate-induced changes in isoprene emissions after the eruption of Mount Pinatubo, *Atmos. Chem. Phys.*, 7, 7117–7125, doi:10.5194/acp-10-7117-2010, 2010.
- Thomason, L. W., Poole, L. R., and Deshler, T.: A Global Climatology Of Stratospheric Aerosol Surface Area Density As Deduced From Stratospheric Aerosol and Gas Experiment II measurements: 1984–1994, *J. Geophys. Res.*, 102, 8967–8976, 1997.
- Thoning, K. W. and Tans, P. P.: Atmospheric Carbon Dioxide at Mauna Loa Observatory 2. Analysis of the NOAA GMCC Data, 1974–1985, *J. Geophys. Res.*, 94, 8549–8565, 1989.
- Valentine, D. W., Holland, E. A., and Schimel, D. S.: Ecosystem and physiological controls over methane production in northern wetlands, *J. Geophys. Res.*, 99, 1563–1571, doi:10.1029/93JD00391, 1994.
- Van Aardenne, J. A., Dentener, F. J., Olivier, J. G. J., Klein Goldewijk, C. G. M., and Lelieveld, J.: A High Resolution Dataset of Historical Anthropogenic Trace Gas Emissions for the Period 1890–1990, *Global Biogeochem. Cy.*, 15, 909–928, 2001.
- Voulgarakis, A., Naik, V., Lamarque, J.-F., Shindell, D. T., Young, P. J., Prather, M. J., Wild, O., Field, R. D., Bergmann, D., Cameron-Smith, P., Cionni, I., Collins, W. J., Dalsøren, S. B., Doherty, R. M., Eyring, V., Faluvegi, G., Folberth, G. A., Horowitz, L. W., Josse, B., McKenzie, I. A., Nagashima, T., Plummer, D. A., Righi, M., Rumbold, S. T., Stevenson, D. S., Strode, S. a., Sudo, K., Szopa, S., and Zeng, G.: Analysis of present day and future OH and methane lifetime in the ACCMIP simulations, *Atmos. Chem. Phys. Discuss.*, 12, 22945–23005, doi:10.5194/acpd-12-22945-2012, 2012.
- Wang, J. S., Logan, J. A., Mcelroy, M. B., Duncan, B. N., Megretskaia, I. A., and Yantosca, R. M.: A 3-D model analysis of the slowdown and interannual variability in the methane growth rate from 1988 to 1997, *Global Biogeochem. Cy.*, 18, GB3011, doi:10.1029/2003GB002180, 2004.
- Wang, Y. and Jacob, D. J.: Anthropogenic forcing on tropospheric ozone and OH since preindustrial times, *J. Geophys. Res.*, 103, 31123–31135, 1998.
- Williams, J. E., Strunk, A., Huijnen, V., and van Weele, M.: The application of the Modified Band Approach for the calculation of on-line photodissociation rate constants in TM5: implications for oxidative capacity, *Geosci. Model Develop.*, 5, 15–35, doi:10.5194/gmd-5-15-2012, 2012.
- Wilton, D. J., Hewitt, C. N., and Beerling, D. J.: Simulated effects of changes in direct and diffuse radiation on canopy scale isoprene emissions from vegetation following volcanic eruptions, *Atmos. Chem. Phys.*, 11, 11723–11731, doi:10.5194/acp-11-11723-2011, 2011.